Double Oxidative Addition Reaction of Dihalomethane to Dinuclear Iridium(I) Complexes: Preparation and Properties of Some Methylene-Bridged Diiridium(III) Complexes. X-ray Structure of $[IrI(\mu\text{-}t\text{-BuS})(CO)(P(OMe)_3]_2[\mu\text{-}CH_2]$

Mohamed El Amane, André Maisonnat, Françoise Dahan, Robert Pince, and René Poilblanc*

Laboratoire de Chimie de Coordination du CNRS associé à l'Université Paul Sabatier, 31400 Toulouse, France

Received August 2, 1984

Thiolato-bridged diiridium(I) complexes $[Ir(\mu\text{-}t\text{-BuS})(CO)L]_2$, **1**, react with dihalomethane to yield quantitatively $[IrX(\mu\text{-}t\text{-BuS})(CO)L]_2[\mu\text{-}CH_2]$, **2** (X = I, L = CO, $P(OMe)_3$, PPh_3, PPh_2Me, PMe_3; X = Br, L = PPh_3). Cis and trans isomers were observed in two cases. A crystal structure determination of $[IrI(\mu\text{-}t\text{-BuS})(CO)(P(OMe)_3]_2(\mu\text{-}CH_2]$ was carried out by X-ray diffraction. The compound crystallizes in orthorhombic space group D_{2h}^{15}—*Pbca* in a cell of dimensions a = 17.033 (3) Å, b = 15.632 (2), and c = 23.808 (3) Å, with Z = 8. On the basis of 3106 unique reflections having $F_o^2 > 4\sigma(F_o^2)$, the structure was refined by full-matrix least-squares technique to conventional agreement indices of R = 0.024 and R_w = 0.027. Each iridium atom is octahedrally coordinated, being bound to one carbonyl, one phosphite, one iodide ligand, two bridging S atoms of the thiolato ligands, and the bridging C atom of the CH_2 group. The phosphite ligands (and the carbonyl ligands) are in a trans arrangement. The *t*-Bu groups are in an anti conformation with respect to the Ir_2S_2 core. The IrIr separation is 3.1980 (4) Å. In solution, complexes **2** undergo syn–anti isomerization on the NMR time scale. The halogen abstraction reaction of **2** by silver(I) salts and the subsequent addition of nucleophilic reagents to the cationic species so obtained are described together with the molecular structure of the products.

Introduction

A large number of μ-alkylidene complexes has now been prepared and characterized.[1] If diazoalkanes remain probably the most versatile precursors for their direct synthesis, the geminal dihalogenoalkane route is of growing interest in their reactions with anionic dimetallic species.[2] On the other hand, very few examples of their direct reaction with neutral organometallic substrates are known. To our knowledge, only two examples have been described so far that apply to the low oxidation state complexes $Au_2(CH_2PMe_2CH_2)_2$[3] and $Pd_2(dppm)_3$.[4]

Following our studies of the reactivity of thiolato-bridged homobimetallic species toward small molecules,[5] we present here the preparation of novel μ-methylene complexes $[IrX(\mu\text{-}t\text{-BuS})(CO)L]_2[\mu\text{-}CH_2]$ (**2**) via quantitative double oxidative addition reactions of dihalomethane with diiridium(I) complexes $[Ir(\mu\text{-}t\text{-BuS})(CO)L]_2$, **1**.

These μ-methylene complexes afford cationic species through halogen abstraction. It is the vacant sites so obtained which make these electron-deficient species, whose reactivity is introduced in this paper, of particular interest.

Experimental Section

General Remarks. All reactions and manipulations were routinely performed under a nitrogen or argon atmosphere in Schlenk-type glassware. All solvents were appropriately dried and freed from molecular oxygen prior to use. Microanalyses were performed by the Service Central d'Analyse du CNRS or by the Service de Microanalyses du Laboratoire de Chimie de Coordination du CNRS. Mass spectra were recorded on a Varian MAT 311 A. Conductivity data were determined for 10^{-3} equiv·L^{-1} solutions in methanol with a commercial conductivity bridge instrument.

Infrared spectra were recorded in hexane or dichloromethane solutions, using a Perkin-Elmer Model 225 grating spectrometer; in the carbonyl stretching region, the spectra were calibrated with water vapor lines. ^1H NMR spectra were obtained at 90 and/or 250 MHz on a Bruker WH 90 FT and/or a Bruker WM 250 FT spectrometer. Chemical shifts were measured with respect of internal tetramethylsilane and are given in parts per million downfield positive.

^{31}P NMR spectra were measured at 36.4 MHz on a Bruker WH 90 FT spectrometer; chemical shifts were measured with respect to external H_3PO_4 and are given in parts per million downfield positive. ^{13}C NMR spectra were recorded at 62.9 MHz on a Bruker WM 250 FT spectrometer; chemical shifts were measured with respect to internal tetramethylsilane and are given in parts per million downfield positive.

Preparation of Compounds. The starting materials $[Ir(\mu\text{-}t\text{-BuS})(CO)_2]_2$, **1a**,[6] and $[Ir(\mu\text{-}t\text{-BuS})(CO)(PR_3)]_2$, **1b–e**,[7] were prepared according to published procedures.

Preparation of $[IrI(\mu\text{-}t\text{-BuS})(CO)_2]_2[\mu\text{-}CH_2]$, 2a. Diiodomethane (0.5 mL) was added to a solution of $[Ir(\mu\text{-}t\text{-BuS})(CO)_2]_2$ (0.300 mg, 0.444 mmol) in hexane (20 mL). A yellow precipitate appeared. After 1 h, the product was filtered off, washed with hexane, and dried in vacuo. The IR spectrum of the filtrate indicated the total consumption of the starting material and the formation of only one product. The product was recrystallized from methanol; electron-impact MS (70 eV), m/e 944 (M^+) plus fragment ions corresponding to successive loss of four CO groups and two I atoms. Anal. Calcd for $C_{13}H_{20}I_2S_2O_4Ir_2$: C, 16.56; H, 2.14. Found: C, 16.55; H, 2.14.

Preparation of $[IrI(\mu\text{-}t\text{-BuS})(CO)(P(OMe)_3)]_2[\mu\text{-}CH_2]$, 2b. Diiodomethane (0.05 mL, 0.63 mmol) was added to a solution of $[Ir(\mu\text{-}t\text{-BuS})(CO)P(OMe)_3]_2$ (0.25 g, 0.29 mmol) in hexane (15 mL). The solution changed within a few minutes from orange to pale

(1) Hermann, W. A. *Adv. Organomet. Chem.* **1982**, *20*, 159–263. Holton, J.; Lappert, M. F.; Pearce, R.; Yarrow, P. I. W. *Chem. Rev.* **1983**, *83*, 135–201.

(2) Sumner, C. E., Jr.; Riley, P. E.; Davis, R. E.; Pettit, R. *J. Am. Chem. Soc.* **1980**, *102*, 1752–1754. Theopold, K. H.; Bergman, R. G. *J. Am. Chem. Soc.* **1983**, *105*, 464–475.

(3) Jandik, P.; Schubert, U.; Schmidbaur, H. *Angew. Chem., Int. Ed. Engl.* **1982**, *21*, 73; *Angew. Chem. Suppl.* **1982**, 1–12.

(4) Balch, A. L.; Hunt, C. T.; Lee, C. L.; Olmstead, M. M.; Farr, J. P. *J. Am. Chem. Soc.* **1981**, *103*, 3764–3772.

(5) Poilblanc, R. *Inorg. Chim. Acta* **1982**, *62*, 75–86.

(6) de Montauzon, D.; Poilblanc, R. *Inorg. Synth.* **1980**, *20*, 237–240.

(7) de Montauzon, D.; Kalck, P.; Poilblanc, R. *J. Organomet. Chem.* **1980**, *186*, 121–130.

(8) Bonnet, J.-J.; Kalck, P.; Poilblanc, R. *Angew. Chem., Int. Ed. Engl.* **1980**, *19*, 551–552. Kalck, P.; Bonnet, J.-J. *Organometallics* **1982**, *1*, 1211–1216.

0276-7333/85/2304-0773$01.50/0

yellow, and a pale yellow precipitate slowly appeared. The precipitate was filtered, washed with petroleum ether, and dried under vacuum (0.24 g, 73%). Anal. Calcd for $C_{17}H_{38}I_2S_2O_8P_2Ir_2$: C, 17.99; H, 3.38. Found: C, 18.32; H, 3.50.

White and yellow crystals were obtained by fractional crystallization on cooling methanol solutions of the pale yellow precipitate at −20 °C. The two products correspond to two isomers of the title compound, α and β, as demonstrated by the X-ray structure determination of the white crystals together with NMR studies of both compounds.

Preparation of [IrI(μ-*t*-BuS)(CO)(PPh_3)]$_2$[μ-CH_2], 2c. Diiodomethane (0.15 mL, 1.86 mmol) was added to an orange-yellow solution of [Ir(μ-*t*-BuS)(CO)(PPh_3)]$_2$ (1.065 g, 0.93 mmol) in dichloromethane (15 mL). The ν(CO) region of the IR spectrum of the solution indicated total consumption of the starting material within a few minutes. The resulting pale yellow solution was concentrated under vacuum. Hexane was added dropwise to precipitate a pale yellow solid. After the mother liquor was decanted, the solid was washed with hexane and dried under vacuum (1.089 g, 83%). The product may be recrystallized from dichloromethane–methanol. Anal. Calcd for $C_{47}H_{50}I_2S_2O_2P_2Ir_2$: C, 40.00; H, 3.58; I, 17.98; S, 4.54. Found: C, 39.95; H, 3.57; I, 17.80; S, 3.74.

Preparation of [IrBr(μ-*t*-BuS)(CO)(PPh_3)]$_2$[μ-CH_2], 2f. This complex was prepared from dibromomethane and [Ir(μ-*t*-BuS)(CO)(PPh_3)]$_2$ by the method used for the preparation of **2c**. The reaction time was much longer, and the IR spectrum of the solution indicated the total transformation of the starting material into the title compound after 25 h.

Preparation of [IrI(μ-*t*-BuS)(CO)(PPh_2Me)]$_2$[μ-CH_2], 2d. This complex was prepared by the procedure used for **2c**, in hexane solution. Anal. Calcd for $C_{37}H_{46}I_2S_2O_2P_2Ir_2$: C, 34.53; H, 3.61; I, 19.72; S, 4.98. Found: C, 34.53; H, 3.54; I, 20.02; S, 4.75.

Preparation of [IrI(μ-*t*-BuS)(CO)(PMe_3)]$_2$[μ-CH_2], 2e. As for **2b**, addition of diiodomethane to an hexane solution of [Ir(μ-*t*-BuS)(CO)(PMe_3)]$_2$ lead to the formation of a pale yellow precipitate within a few minutes. Anal. Calcd for $C_{17}H_{38}I_2S_2O_2P_2Ir_2$: C, 19.65; H, 3.69; I, 24.43; S, 6.17. Found: C, 19.61; H, 3.73; I, 24.49; S, 5.62.

Two kinds of crystals were obtained by fractional crystallization on cooling methanol solutions of the pale yellow precipitate, corresponding to two isomers of the title compound.

Reaction of [IrI(μ-*t*-BuS)(CO)($P(OMe)_3$)]$_2$ with Diazomethane. [IrI(μ-*t*-BuS)(CO)($P(OMe)_3$)]$_2$ (0.2 mmol) prepared according to the published method,[8] placed in the outside tube of an Aldrich MNNG diazomethane kit, was allowed to react at 0 °C with diazomethane produced by 0.3 g (2.25 mmol) of *N*-methyl-*N'*-nitro-*N*-nitrosoguanidine and 1.5 mL of 5 N sodium hydroxide. No reaction was detected after 20 h, as indicated by the IR spectrum.

Reaction of Complexes 2 with Silver(I) Salts. Preparation of {[Ir(μ-*t*-BuS)(CO)$_2$(PPh_3)]$_2$[μ-CH_2]}$^{2+}$(ClO_4^-)$_2$, 6a, and IR Characterization of [(CO)$_2$IIr(μ-*t*-BuS)$_2$(μ-CH_2)Ir(CO)$_2$]$^+$$ClO_4^-$, 3a, {[Ir($\mu$-*t*-BuS)(CO)$_2$]$_2$[$\mu$-$CH_2$]}$^{2+}$[$ClO_4^-$]$_2$, 4a, and [(CO)$_2$IIr($\mu$-*t*-BuS)$_2$($\mu$-BuS)$_2$($\mu$-$CH_2$)Ir(CO)$_2$($PPh_3$)]$^+$$ClO_4^-$, 5a. A solution of [IrI(μ-*t*-BuS)(CO)$_2$]$_2$[μ-CH_2], **2a** (0.200 g, 0.21 mmol), in dichloromethane (15 mL) was allowed to react with $AgClO_4$ (0.09 g, 0.43 mmol) in suspension at 0 °C. IR spectra were periodically run over a period of 6 h. In the ν(CO) region, the absorptions of the starting material **2a** at 2111, 2102, and 2062 cm^{-1} progressively decreased and two sets of new absorptions appeared. A first set of absorptions at 2130, 2115, and 2084 cm^{-1}, attributable to the intermediate monocationic species **3a**, first grew in and then disappeared. A second set of absorptions at 2143, 2132, and 2098 cm^{-1}, attributable to the dication **4a**, slowly grew in until the complete disappearance of the starting material **2a** and of the intermediate **3a**. After 6 h, the spectrum exhibited the three bands of **4a**, and later on no significant changes were observed. The solution was filtered and then triphenylphosphine (0.110 g, 0.42 mmol) was added to the filtrate at room temperature. The changes in the IR spectrum indicated the formation of a new complex, **6a**, having three ν(CO) bands at 2104, 2093, and 2049 cm^{-1}. The yellow solution was concentrated under reduced pressure, and petroleum ether was added. Crystallization at −20 °C gave yellow crystals (0.240 g, 80%): conductivity, Λ = 193 $\Omega^{-1}\cdot cm^2\cdot mol^{-1}$. Anal. Calcd for $C_{49}H_{50}Cl_2O_2P_2S_2Ir_2$: C, 41.67; H, 3.57. Found: C, 41.11; H, 3.28.

6a may also be prepared by the simultaneous action of $AgClO_4$ and PPh_3 on a solution of **2a** in dichloromethane. Monitored by IR over a period of 6 h, the spectra indicated the slow formation of **6a** together with the formation and the disappearance of a monocationic intermediate, **5a**, having three ν(CO) bands at 2115, 2105, and 2067 cm^{-1}.

Preparation of {[Ir(μ-*t*-BuS)(CO)$_2$($P(OMe)_3$)]$_2$[μ-CH_2]}$^{2+}$(ClO_4^-)$_2$, 6b, and IR Characterization of {[Ir(μ-*t*-BuS)(CO)($P(OMe)_3$)]$_2$[μ-CH_2]}$^{2+}$(ClO_4^-)$_2$, 4b, and [(CO)($P(OMe)_3$)IIr(μ-*t*-BuS)$_2$(μ-CH_2)Ir($P(OMe)_3$)(CO)$_2$]$^+$$ClO_4^-$, 5b. A solution of the white α isomer of **2b** (0.305 g, 0.27 mmol) in dichloromethane (20 mL) was allowed to react with $AgClO_4$ (0.115 g, 0.55 mmol) at room temperature. After 2 h, the initial compound **2b** was consumed and the IR spectrum indicated the presence of a new compound, **4b**, having a single broad ν(CO) band at 2069 cm^{-1}. The solution was filtered, and the filtrate then was allowed to react with carbon monoxide at room temperature and atmospheric pressure. The changes in the IR spectrum indicated the formation of a new complex, **6b**, having three ν(CO) bands at 2112, 2080, and 2065 cm^{-1}, after a reaction time of 30 min. The solution was concentrated under reduced pressure and methanol was added.

Crystallization at −20 °C gave pale yellow crystals of **6b** (0.191 g, 62%): conductivity, Λ = 225 $\Omega^{-1}\cdot cm^2\cdot mol^{-1}$. Anal. Calcd for $C_{19}H_{38}Cl_2O_{18}P_2S_2Ir_2$: C, 20.09; H, 3.37. Found: C, 19,87; H, 3.84.

6b may also be prepared by the simultaneous action of silver perchlorate and carbon monoxide on a solution of **2b** in dichloromethane. Under these conditions, the intermediate **5b**, having ν(CO) bands at 2115, 2070, and 2055 cm^{-1}, was detected.

Preparation of {[Ir(μ-*t*-BuS)(CO)($P(OMe)_3$)$_2$]$_2$[μ-CH_2]}$^{2+}$(ClO_4^-)$_2$ 6b′. A solution of **2b** (0.250 g, 0.22 mmol) in dichloromethane (15 mL) was allowed to react simultaneously with $AgClO_4$ (0.091 g, 0.44 mmol) and $P(OMe)_3$ (5 μL, 0.44 mmol). After 2 h, the initial compound **2b** was consumed and the IR spectrum indicated the presence of a new compound **6b′** having two ν(CO) bands at 2069 and 2059 cm^{-1}. The solution was filtered, and the filtrate was concentrated under reduced pressure to about 7 mL. Methanol (7 mL) was added to the residue. Crystallization at −20 °C gave white crystals of **6b′** (0.205 g, 70%): conductivity, Λ = 219 $\Omega^{-1}\cdot cm^2\cdot mol^{-1}$. Anal. Calcd for $C_{23}H_{56}Cl_2O_{22}P_4S_2Ir_2$: C, 20.80; H, 4.25. Found: C, 20.73; H, 4.06.

Preparation of {[Ir(μ-*t*-BuS)(CO)$_2$(PPh_3)]$_2$[μ-CH]}$^{2+}$(PF_6^-)$_2$, 6c, and IR Characterization of {[Ir(μ-*t*-BuS)(CO)(PPh_3)]$_2$-[μ-CH_2]}$^{2+}$(PF_6^-)$_2$, 4c. $AgPF_6$ (0.182 g, 0.72 mmol) was added to a solution of **2c** (0.512 g, 0.36 mmol) in dichloromethane (15 mL) at room temperature. After 1 h the initial compound **2c** was consumed and the IR spectrum indicated the presence of a new compound **4c** having a ν(CO) band at 2034 cm^{-1}. The solution was filtered, and the filtrate then was allowed to react with carbon monoxide at room temperature and atmospheric pressure. After a reaction time of 15 min, the IR spectrum indicated the total conversion of **4c** into a new compound **6c** having ν(CO) bands at 2081, 2041, and 2016 cm^{-1}. The solution then was concentrated under reduced pressure to half its volume, and methanol was added. Crystallization at −20 °C gave **6c** as a yellow solid (0.295 g, 54%): conductivity, Λ = 188 $\Omega^{-1}\cdot cm^2\cdot mol^{-1}$. Anal. Calcd for $C_{49}H_{50}F_{12}O_4P_4S_2Ir_2$: C, 39.15; H, 3.35. Found: C, 39.34; H, 3.33.

Crystal and Molecular Structure Determination of the α Isomer of 2b. White parallelepipedic air-stable crystals were obtained by slow cooling of a methanol solution of **2b** to −20 °C. Preliminary film data on Weissenberg cameras indicated orthorhombic Laue symmetry. The observed systematic extinctions lead to the *Pbca* space group. Data collection was carried out on a CAD 4 Enraf-Nonius diffractometer. The final crystal parameters and the details of the data collection procedure are given in Table I.

Structure Solution and Refinement. The structure was solved[9] by the heavy-atom technique. A Patterson map yielded positions for Ir and I atoms. Subsequent Fourier maps revealed the positions of all non-hydrogen atoms, which were refined an-

(9) Sheldrick, G. M. "Shelx 76", Program for Crystal Structure Determination; University of Cambridge: Cambridge, England, 1976.

Scheme I

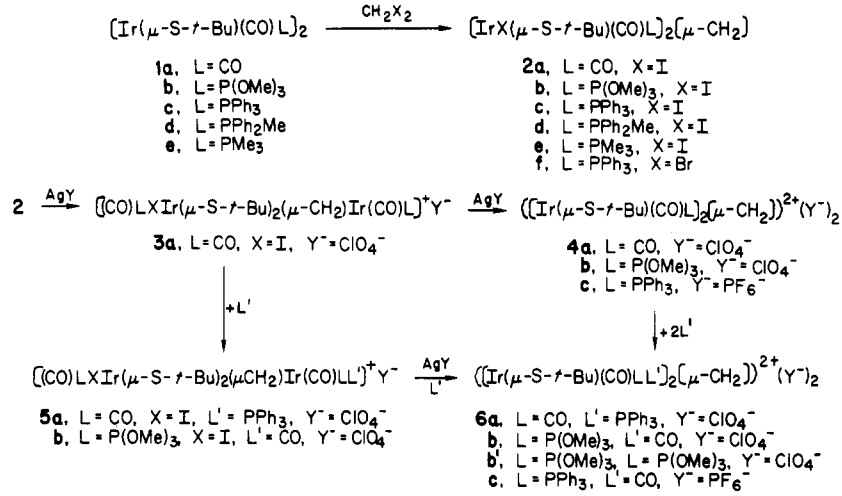

Table I. Crystal Data and Experimental Details of the X-ray Diffraction Study of 2b

Crystal Parameters at 20 °C[a]	
formula	$C_{17}H_{38}I_2O_8P_2S_2Ir_2$
fw	1134.81
cell parameters	
a, Å	17.033 (3)
b, Å	15.632 (2)
c, Å	23.808 (3)
V, Å^3	6339.1
cryst system	orthorhombic
absences	$0kl$, $k = 2n + 1$; $h0l$, $l = 2n + 1$; $hk0$, $h = 2n + 1$
space group	D_{2h}^{15}—*Pbca*
Z	8
d(calcd), g/cm^3	2.378
d(obsd), g/cm^3	2.25 (by flotation in 1,1,2,2-tetrabromoethane/1,2-dichlorobenzene)
F(000)	4208
Measurement of Intensity Data	
cryst dimens, mm	0.150 × 0.275 × 0.100
radiation	Mo K$\bar{\alpha}$ from graphite monochromatization
receiving aperture	4.0 × 4.0 mm; 30 cm from crystal
takeoff angle, deg	2.4
scan mode	ω–2θ
scan range, deg	0.70 + 0.35 tan θ
2θ limits, deg	51
intensity std[b]	3 reflctns every 7200 s
no. of independent reflectns collected	5686
Treatment of Intensity Data	
reductn to F_o^2 and $\sigma(F_o^2)$	corr for bkgds, attenuators and Lorentz-polarization in the usual manner
linear abs coeff μ, cm^{-1}	105.5
absorption corr[c]	$T_{max} = 0.374$; $T_{min} = 0.162$
obsd unique data ($F_o^2 \geq 4\sigma(F_o^2)$)	3106
no. of variables	298
$R = \Sigma \|\|F_o\| - \|F_c\|\| / \Sigma \|F_o\|$	0.024
$R_w = (\Sigma w(\|F_o\| - \|F_c\|)^2 / \Sigma w F_o^2)^{1/2}$	0.027
w	$1/[\sigma^2(F_o) + (pF_o)^2]$
p	0.013

[a] From a least-squares fitting of the setting angles of 25 reflections. [b] Showed only random, statistical fluctuations. [c] Coppens, P.; Leiserowitz, L. Rabinovitch, D. *Acta Crystallogr.* **1965**, *18*, 1035–1038.

isotropically. The hydrogen atoms were localized on a difference Fourier map and introduced in the last cycles of refinement with constrained geometry (C–H = 0.95 Å; H–C–H = 109.5°) with an isotropic thermal parameter $U = 0.06$ Å^2.

Table II. Final Least-Squares Atomic Coordinates with Estimated Standard Deviations for 2b

atom	*x/a*	*y/b*	*z/c*
Ir(1)	0.53778 (2)	0.27803 (2)	0.62689 (1)
Ir(2)	0.43050 (2)	0.20085 (2)	0.52899 (1)
I(1)	0.49560 (5)	0.36939 (5)	0.72389 (3)
I(2)	0.26713 (4)	0.20235 (5)	0.51271 (3)
C(1)	0.6172 (6)	0.3559 (7)	0.6128 (4)
O(1)	0.6616 (4)	0.4097 (5)	0.6049 (3)
C(2)	0.4222 (6)	0.0851 (8)	0.5142 (4)
O(2)	0.4136 (4)	0.0144 (5)	0.5027 (3)
C(17)	0.5493 (4)	0.2018 (6)	0.5548 (3)
S(1)	0.41500 (12)	0.20025 (14)	0.63010 (9)
C(9)	0.4092 (5)	0.0935 (6)	0.6642 (4)
C(10)	0.3303 (6)	0.0546 (7)	0.6433 (4)
C(11)	0.4044 (6)	0.1095 (7)	0.7266 (4)
C(12)	0.4752 (5)	0.0333 (6)	0.6491 (4)
S(2)	0.46355 (14)	0.34705 (15)	0.55123 (10)
C(13)	0.3841 (6)	0.4252 (6)	0.5667 (5)
C(14)	0.3272 (6)	0.3947 (7)	0.6114 (5)
C(15)	0.4278 (6)	0.5062 (6)	0.5860 (4)
C(16)	0.3432 (6)	0.4419 (7)	0.5112 (4)
P(1)	0.62418 (14)	0.20089 (18)	0.67810 (11)
O(3)	0.5908 (4)	0.1620 (4)	0.7341 (3)
C(3)	0.6332 (7)	0.1018 (8)	0.7683 (4)
O(4)	0.6607 (4)	0.1191 (4)	0.6491 (3)
C(4)	0.7177 (6)	0.1214 (7)	0.6061 (5)
O(5)	0.7025 (4)	0.2489 (5)	0.6950 (3)
C(5)	0.7126 (8)	0.3102 (8)	0.7376 (6)
P(2)	0.45785 (14)	0.22468 (17)	0.43780 (10)
C(6)	0.5461 (4)	0.2442 (4)	0.4241 (3)
C(6)	0.5993 (6)	0.1904 (9)	0.3994 (6)
O(7)	0.4153 (4)	0.3063 (4)	0.4143 (3)
C(7)	0.4301 (6)	0.3366 (8)	0.3582 (4)
O(8)	0.4423 (4)	0.1493 (4)	0.3951 (3)
C(8)	0.3673 (6)	0.1213 (8)	0.3772 (5)

Neutral atom scattering factors for non-hydrogen atoms and corrections for anomalous dispersion effects for Ir, I, S, and P atoms were obtained from the tabulation of Cromer and Waber.[10] Scattering factors for the hydrogen atoms were those of Stewart et al.[11] The final cycle of refinement lead to $R = 0.024$ and $R_w = 0.027$. The weighting scheme used in the minimization of the function $\sum w(|F_o| - |F_c|)^2$ is defined as $w = 1/\sigma^2(F_o) + (pF_o)^2$ where p is the factor to prevent overweighting of strong reflections. An analysis of variance according to F_o and $(\sin\theta)/\lambda$ showed satisfactory consistency. Atomic positional parameters with their

(10) Cromer, D. T.; Waber, J. T. "International Tables for X-ray Crystallography"; Kynoch Press: Birmingham, England, 1974; Vol. IV, Table 2.2B, p 99. Cromer, D. T. *Ibid.* Table 2.3.1, p 149.
(11) Stewart, R. F.; Davidson, E. R.; Simpson, W. T. *J. Chem. Phys.* **1965**, *42*, 3175–3187.

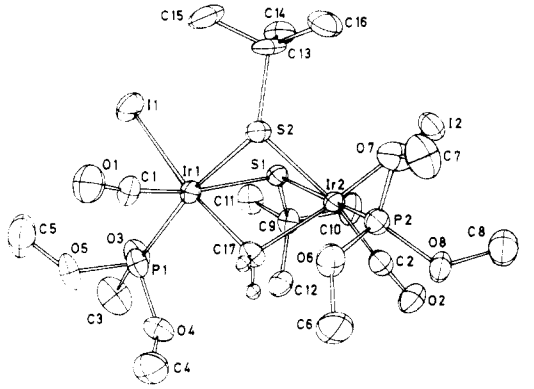

Figure 1. A perspective representation of $[IrI(\mu\text{-}t\text{-}BuS)(CO)(P(OMe)_3)]_2[\mu\text{-}CH_2]$, **2b**. The vibrational ellipsoids are drawn at the 40% probability level. Methylene hydrogens are drawn at an arbitrary scale.

standard deviations are reported in Table II.

Results and Discussion

The addition of diiodomethane to the complexes $[Ir(\mu\text{-}t\text{-}BuS)(CO)L]_2$, **1a–e**, in stoichiometric quantities as well as in large excess, in dichloromethane or hexane solution at room temperature lead readily and quantitatively to (μ-methylene)diiridium(III) (1/1) adducts $[IrI(\mu\text{-}t\text{-}BuS)(CO)L]_2[\mu\text{-}CH_2]$, **2a–e** (Scheme I). No intermediates or byproducts were detected in solution. During the reaction times, no reactions between the starting diiridium(I) materials and dichloromethane were observed. Dibromomethane reacts much more slowly and a bromo analogue adduct, **2f**, was obtained in the case where L = PPh_3 after a reaction time of 25 h.

Contrasting with the addition of CH_2I_2 to **1a,c,d**, which gives 1/1 single adducts, the addition of CH_2I_2 to **1b,e** yields a mixture of two isomeric adducts, α and β. Monitored by proton NMR, the addition of CH_2I_2 to **1b** in equimolar quantities leads to a mixture of the α and β isomers in the ratio $[\alpha]:[\beta] = 1:2$. The relative concentration of α and β isomers in solution is remarkably stable and the $[\alpha]:[\beta]$ ratio remains unchanged even after several weeks. Pure α isomer was obtained by fractional crystallization as white parallelepipedic crystals. We did not succeed in preparing the pure β isomer, and the corresponding solid products of fractional crystallizations always contained traces of the α isomer. No conversion of one isomer into the other occurred, even upon heating for hours in refluxing hexane.

These adducts form air-stable, pale yellow or white solids which dissolve readily in dichloromethane and tetrahydrofuran, to a lesser extent in toluene or methanol and are slightly soluble in petroleum ether. The structure of these new compounds has been resolved by an X-ray diffraction analysis (in the case of **2b**), elemental analyses, a mass spectrum (in the case of **2a**), IR spectra, and ^1H, ^{13}C, and ^{31}P NMR studies at room temperature and at low temperature. They correspond to double oxidative addition of dihalomethane to the diirium(I) complexes. They may also be regarded formally as carbene adducts of the diiodo diiridium(II) complexes $[IrI(\mu\text{-}t\text{-}BuS)(CO)L]_2$(*Ir–Ir*), described previously.[8] Nevertheless, attempts to prepare **2b** by reaction between $[IrI(\mu\text{-}t\text{-}BuS)(CO)(P(OMe)_3)]_2$, for instance, and diazomethane have been unsuccessful.

Crystal Structure of the α Isomer of 2b. The crystal structure of the α isomer of **2b** consists of the packing of well-separated dinuclear molecules. Figure 1 shows a view of the molecule with the atom numbering scheme. Bond distances are given in Table III and bond angles in Table IV.

Table III. Selected Interatomic Distances (Å) with Esd's for 2b

Ir(1)-Ir(2)	3.1980 (4)		
Ir(1)-S(1)	2.420 (2)	Ir(2)-S(1)	2.422 (2)
Ir(1)-S(2)	2.451 (2)	Ir(2)-S(2)	2.412 (2)
Ir(1)-P(1)	2.260 (3)	Ir(2)-P(2)	2.251 (2)
Ir(1)-C(1)	1.850 (10)	Ir(2)-C(2)	1.848 (12)
Ir(1)-I(1)	2.8087 (8)	Ir(2)-I(2)	2.8096 (8)
Ir(1)-C(17)	2.099 (8)	Ir(2)-C(17)	2.115 (7)
P(1)-O(3)	1.571 (7)	P(2)-O(6)	1.569 (7)
P(1)-O(4)	1.580 (7)	P(2)-O(7)	1.571 (7)
P(1)-O(5)	1.583 (7)	P(2)-O(8)	1.579 (7)
O(3)-C(3)	1.438 (13)	O(6)-C(6)	1.368 (14)
O(4)-C(4)	1.413 (13)	O(7)-C(7)	1.438 (12)
O(5)-C(5)	1.404 (15)	O(8)-C(8)	1.416 (12)
C(1)-O(1)	1.147 (13)	C(2)-O(2)	1.149 (14)
S(1)-C(9)	1.858 (9)	S(2)-C(13)	1.860 (10)
C(9)-C(10)	1.557 (13)	C(13)-C(14)	1.517 (15)
C(9)-C(11)	1.509 (13)	C(13)-C(15)	1.538 (14)
C(9)-C(12)	1.510 (13)	C(13)-C(16)	1.518 (15)

Table IV. Selected Bond Angles (deg) with Esd's for 2b

S(1)-Ir(1)-S(2)	78.38 (8)	S(1)-Ir(2)-S(2)	79.10 (8)
S(1)-Ir(1)-P(1)	106.12 (8)	S(1)-Ir(2)-P(2)	169.02 (8)
S(1)-Ir(1)-C(1)	165.4 (3)	S(1)-Ir(2)-C(2)	100.2 (3)
S(1)-Ir(1)-I(1)	90.48 (5)	S(1)-Ir(2)-I(2)	91.67 (5)
S(1)-Ir(1)-C(17)	79.7 (2)	S(1)-Ir(2)-C(17)	79.4 (2)
S(2)-Ir(1)-P(1)	165.32 (9)	S(2)-Ir(2)-P(2)	90.38 (9)
S(2)-Ir(1)-C(1)	87.4 (3)	S(2)-Ir(2)-C(2)	170.7 (3)
S(2)-Ir(1)-I(1)	104.39 (6)	S(2)-Ir(2)-I(2)	104.68 (6)
S(2)-Ir(1)-C(17)	72.4 (2)	S(2)-Ir(2)-C(17)	72.9 (2)
P(1)-Ir(1)-C(1)	88.5 (3)	P(2)-Ir(2)-C(2)	89.6 (3)
P(1)-Ir(1)-I(1)	89.67 (7)	P(2)-Ir(2)-I(2)	94.04 (6)
P(1)-Ir(1)-C(17)	94.4 (2)	P(2)-Ir(2)-C(17)	94.6 (2)
C(1)-Ir(1)-I(1)	90.1 (3)	C(2)-Ir(2)-I(2)	84.6 (3)
C(1)-Ir(1)-C(17)	99.0 (4)	C(2)-Ir(2)-C(17)	97.8 (4)
I(1)-Ir(1)-C(17)	170.1 (2)	I(2)-Ir(2)-C(17)	171.0 (2)
Ir(1)-S(1)-Ir(2)	82.67 (7)	Ir(1)-S(2)-Ir(2)	82.22 (7)
Ir(1)-S(1)-C(9)	120.7 (3)	Ir(1)-S(2)-C(13)	121.2 (3)
Ir(2)-S(1)-C(9)	116.3 (3)	Ir(2)-S(2)-C(13)	119.7 (3)
Ir(1)-C(17)-Ir(2)	98.7 (3)		
Ir(1)-C(1)-O(1)	174.0 (9)	Ir(2)-C(2)-O(2)	176.0 (8)

Part of the molecule recalls the thiolato-bridged diiridium entity found in the starting material $[Ir(\mu\text{-}t\text{-}BuS)(CO)(P(OMe)_3)]_2$,[12] and the methylene group coming from the added diiodomethane occupies a bridging position between the iridium atoms. The iodide ligands, one on each iridium in a terminal mode, are mutually trans to the bridging methylene. Each iridium atom lies in a distorted octahedral environment, both octahedra sharing the face [S(1),S(2),C(17)]. The *tert*-butyl groups of the thiolato bridging ligands are in an anti conformation with respect to the Ir_2S_2 core, whereas the carbonyl ligands and the phosphite ligands occupy positions which confer a trans conformation to the molecule. I(1) and I(2) atoms are slightly out of the plane [Ir(1),Ir(2),C(17)]. They are 0.2172 (8) and 0.2162 (8) Å away from this plane, respectively, and are located on the same side. This is probably due to the proximity of the bulky *tert*-butyl group around the C(13) atom which is in exo position and which is located on the other side of the plane [Ir(1),Ir(2),C(17)]. The Ir···Ir distance is 3.1980 (4) Å, and the dihedral angle between the two planes containing [Ir(1),S(1),S(2)] and [Ir(2),S(1),S(2)] is 117.0°. When compared with the corresponding data found in the starting material **1b**, i.e., 3.216 (2) Å and 123.2°,[12] these values, together with Ir–S distances and Ir–S–Ir and S–Ir–S angles, show that the geometry of the central Ir_2S_2 core of **1b** is only slightly affected when CH_2I_2 is added (Figure 2). In agreement with other observations,1 the rather large Ir(1)–C(17)–Ir(2) angle of 98.7 (3)°

(12) Bonnet, J.-J.; Thorez, A.; Maisonnat, A.; Galy, J.; Poilblanc, R. *J. Am. Chem. Soc.* **1979**, *101*, 5940–5948.

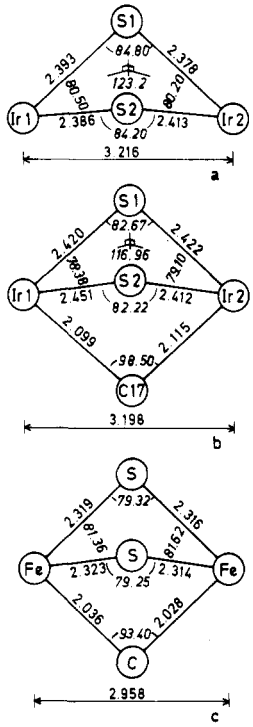

Figure 2. Schemes of the M_2S_2 and M_2S_2C cores (M = Ir or Fe) in compounds $[Ir(\mu\text{-}t\text{-BuS})(CO)(P(OMe)_3)]_2$, **1b** (from ref 12), $[IrI(\mu\text{-}t\text{-BuS})(CO)(P(OMe)_3)]_2[\mu\text{-}CH_2]$, **2b**, and $[Fe(\mu\text{-S-Me})(CO)_3]_2[\mu\text{-}C(F)(CF_3)]$(from ref 13).

Table V. Infrared Spectra[a] for Complexes 2-6

compd	isomer	ν(CO), cm^{-1}
2a		2111 vs, 2102 s, 2062 vs
2b	α	2048 sh, 2038 vs
2b	β	2040 vs, 2030 sh
2c	α	2030 sh, 2016 vs
2d	α	2018 vs, 2020 sh, 2016 vs, 2028 s[b]
2e	α	2028 vs, 2020 sh
2e	β	2027 sh, 2019 vs
2f	α	2030 sh, 2018 vs
3a		2130 s, 2115 s, 2084 vs
4a		2143 s, 2132, 2098 vs
4b		2069 br
4c		2034 br
5a		2115 s, 2105 s, 2067 s
5b		2115 s, 2070 vs, 2055 s
6a		2104 vs, 2093 s, 2049 vs
6b		2112 vs, 2080 vs, 2065 vs
6b′		2069 vs, 2059 sh
6c		2081 s, 2041 vs br, 2016 sh

[a] Run in CH_2Cl_2; s = strong, vs = very strong, sh = shoulder, br = broad. α and β refer to the two isomeric forms discussed in the text.

is consistent with the methylene group bridging two nonbonded iridium atoms and compares well (Figure 2) with that found in the case of the isoelectronic and isostructural diiron(II) neutral complex $[Fe(CO)_3(\mu\text{-SMe})]_2[\mu\text{-}C(F)(CF_3)]$, i.e., 93.4° ($d$(Fe–Fe) = 2.958 (1) Å).[13]

Molecular Structure of Complexes 2. IR data of complexes **2a–f** are presented in Table V. Addition of CH_2I_2 or CH_2Br_2 to complexes **1** is accompanied by a shift of ca. 60–80 cm^{-1} of the ν(CO) bands toward higher frequencies, as expected, in fact, for two-electron oxidative addition processes on each iridium(I) centers.

^1H and ^{31}P NMR characteristics of complexes **2** are collected in Table VI and VII. The ^1H and ^{31}P NMR

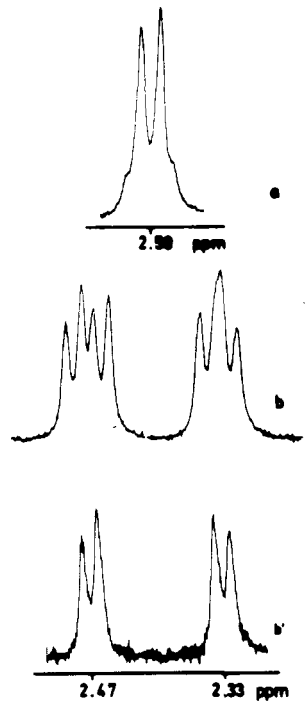

Figure 3. 250-MHz ^1H NMR spectra (CD_2Cl_2) of the α isomer of **2b** in the bridging methylene region: (a) at 298 K; (b) at 213 K; (b′) $^1H\{^{31}P\}$ at 213 K.

Scheme II

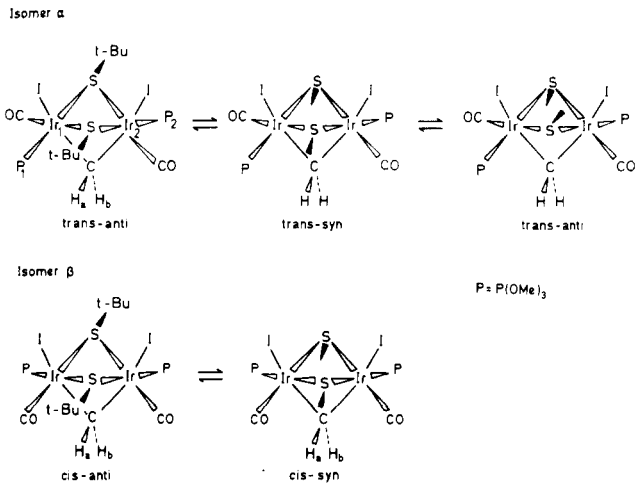

spectra of the α isomer of **2b** are temperature dependent. In the slow-exchange region, i.e., at 213 K, these spectra are in agreement with the trans-anti conformation observed in the solid state. The ^1H NMR spectrum which exhibits two singlets of equal intensity at 1.63 and 1.42 ppm reveals nonequivalent *tert*-butyl groups consistent with their mutual anti disposition. As expected, the $^{31}P\{^1H\}$ spectrum which exhibits two doublets of equal intensity at 65.24 and 63.34 ppm, with doublet spacings of 4.4 Hz, reveals nonequivalent and mutually coupled phosphorus nuclei for the phosphite ligands. On the ^1H NMR spectrum, the phosphite protons appear as two doublets of equal intensity at 3.81 and 3.82 ppm with J_{PH} coupling of 11.3 Hz in both cases. By decoupling the phosphorus nuclei, the methylene resonances appear at 2.47 and 2.33 ppm, as a typical AB pattern (Figure 3b′) with a ca. 4.2 Hz coupling between the geminal protons. Further splitting occurs due to P–H couplings, and the spectrum shown in Figure 3b is interpreted as a poorly resolved AB part of an ABXY spin system, in the first-order approximation,[14] with one of the P–H couplings for each meth-

(13) Bonnet, J.-J.; Mathieu, R.; Poilblanc, R.; Ibers, J. A. *J. Am. Chem. Soc.* **1979**, *101*, 7487–7496.

Table VI. ^1H NMR[a] Data for Complexes 2

compd	isomer	T, K	δ(PR$_3$)	δ(μ-S-t-Bu)	δ(μ-CH$_2$)		
2a		298		1 69 (s, br)		2.49 (s br)	
2a		253		1.79 (s) 1.59 (s)	AB	2.57 2.45	$^2J_{HH}$ = 5.6
2b	α	298	3.87 (d, $^3J_{PH}$ = 11.5)	1.61 (br)	AA'XX'	2.50 ($^3J_{PH}$ = 5.2)	
2b	α	213	3.81 (d, $^3J_{PH}$ = 11.3) 3.82 (d, $^3J_{PH}$ = 11.3)	1.63 (s) 1.42 (s)	ABXY	2.47 ($^3J_{PH}$ = 7.7) 2.33 ($^3J_{PH}$ = 6.0)	$^2J_{HH}$ = 4.2
2b	β	298	3.86 (d, $^3J_{PH}$ = 11.0)	1.69 (s) 1.56 (t, $^5J_{PH}$ = 0.7)	ABX_2	2.60 ($^3J_{PH}$ = 0.8) 2.49 ($^3J_{PH}$ = 7.6)	$^2J_{HH}$ = 4.2
2b	β	213	3.80 (d, $^3J_{PH}$ = 11.0)	1.61 1.48	ABX_2	2.64 2.31 ($^3J_{PH}$ = 7.6)	$^2J_{HH}$ = 4.2
2c	α[b]	298	7.42 (m) 7.76 (m)	1.39 (s)	AA'XX'	1.34 ($^3J_{PH}$ = 7.0)	
2c	α[b]	203		1.27 (vbr)	d		
2d	α[b]	298	δ(Me) 2.60 (d, $^3J_{PH}$ = 11.0)	1.55 (s)	AA'XX'	1.35 ($^3J_{PH}$ = 7.0)	
2e	α[b]	298	1.89 (d, $^3J_{PH}$ = 10.6)	1.62 (s)	AA'XX'	2.21 ($^3J_{PH}$ = 8.0)	
2e	β[b]	298	1.78 (d, $^3J_{PH}$ = 11.0)	1.68 (s) 1.57 (s)		2.46[c]	
2f	α[b] 2	298	7.39 (m), 7.76 (m)	1.42 (s)			

[a] Run in CD_2Cl_2 at 250 MHz unless otherwise indicated; δ and J (Hz); s = singlet, d = doublet, t = triplet, m = multiplet, br = broad; α and β refer to the two isomeric forms discussed in the text. [b] Recorded at 90 MHz. [c] Poorly resolved multiplet. [d] Hidden by the broad *tert*-butyl singlet.

Table VII. $^{31}P\{^1H\}$[a] and ^{13}C[b] NMR Data for Complexes 2 and 6[c]

compd	isomer	T, K	δ(^{31}P)	δ(μ-CH$_2$)	$^1J_{CH}$, Hz
2a		298		−34.76 (t)	151
2b	α	298	62.40 (s)	−28.87 (t)	149
2b	α	213	65.24 (d) 63.34 (d) ($^4J_{PP}$ = 4.4)		
2b	β	298	62.15 (s)	−29.56 (t)	147
2b	β	213	64.01 (s)		
2c	α	298	−7.91 (s)	−16.20 (t)	147
2c	α	193	1.25 (br) −13.16 (br)		
2f	α	298	−10.33 (s)		
6a		298	−0.4 (s)	−46.07 (t)[d]	$^2J_{CP}$ = 7.3
6b′		298	93.72[e] 61.26 (AA'XX')	−48.74 (t)[d]	$^2J_{CP}$ = 10.5
6b				−38.18[d]	
6c				−66.72[d]	

[a] At 36.4 MHz. [b] At 62.9 MHz. [c] Run in $CDCl_3$; s = singlet, d = doublet, t = triplet, br = broad. α and β refer to the two isomeric forms discussed in the text. [d] $^{13}C\{^1H\}$. [e] See Figure 5.

ylene proton, H_a and H_b, weaker than 1 Hz. We assign these weak couplings to $^3J_{H_aP_1}$ and $^3J_{H_bP_2}$ (Scheme II) and the couplings of 7.7 and 6.0 Hz to $^3J_{H_aP_2}$ and $^3J_{H_bP_1}$. The relative disposition of H_a, C, Ir_2, and P_2 atoms (the torsion angle H_a–C–Ir_2–P_2 is 157°) might be expected to give larger $^3J_{HP}$ coupling than the relative disposition of H_b, C, Ir_2, and P_2 atoms (the torison angle H_b–C–Ir_2–P_2 is 79°).[16]

Upon raising the temperature from 213 to 298 K, the phosphorus ligands become equivalent, as indicated by the coalescence of their $^{31}P\{^1H\}$ and ^1H signals into a single singlet at 62.4 ppm and a single doublet at 3.88 ppm, respectively. Similarly, the *tert*-butyl groups become equivalent: their singlets coalesce into a single broad singlet at 1.61 ppm. The A and B parts of the ABXY spin system for the methylene protons coalesce into a virtual doublet (Figure 3a) interpreted as the envelope of the A part of an AA'XX' spin system in which the X nuclei are mutually weakly coupled.

This fluxional behavior of the α isomer of **2b** on the NMR time scale may be interpreted in terms of a syn–anti dynamic equilibrium due to an intramolecular endo–exo exchange of the alkylthiolato groups currently observed, for example, in isoelectronic diiron(II) complexes, $[RSFe(CO)(C_5H_5)]_2$.[18] This process is schematically shown on Scheme II.

The β isomer of **2b** exhibits only one singlet at 62.15 ppm, at 298 K as at 213 K, in the $^{31}P\{^1H\}$ NMR spectra. In the ^1H NMR spectra, it exhibits one doublet at 3.80 ppm for the phosphite protons, at 298 K as at 213 K, and, more significantly, one singlet at 1.69 ppm and one triplet at 1.56 ppm (with triplet spacings of 0.7 Hz) of equal intensities for the *tert*-butyl protons. A relative cis disposition of both carbonyl groups and of both phosphite ligands is then necessarily required for this isomer in which the *tert*-butyl group resonating at higher chemical shift

(14) The chemical shift differences δ_{AB} and δ_{XY}, 35 and 70 Hz, respectively, may be considered as large compared to coupling constants J_{AB} and J_{XY}, 4.2 and 4.4 Hz, respectively, so that the first-order approximation is valid.[15]

(15) Abraham, R. J.; Bernstein, H. J. *Can. J. Chem.* **1961**, *39*, 216–230.

(16) A Karplus-type dependence of the $^3J_{P-Ir-C-H}$ on the torsion angle is assumed, which is similar to that invoked[17] for the $^3J_{Pt-P-C-H}$ in the case of heterodinuclear platinum–palladium complexes containing the bis(diphenylphosphino)methane bridging ligand.

(17) McEwan, D. M.; Pringle, P. G.; Shaw, B. L. *J. Chem. Soc., Chem. Commun.* **1982**, 859–861.

(18) Dekker, M.; Knox, G. R.; Robertson, C. G. *J. Organomet. Chem.* **1969**, *18*, 161–167.

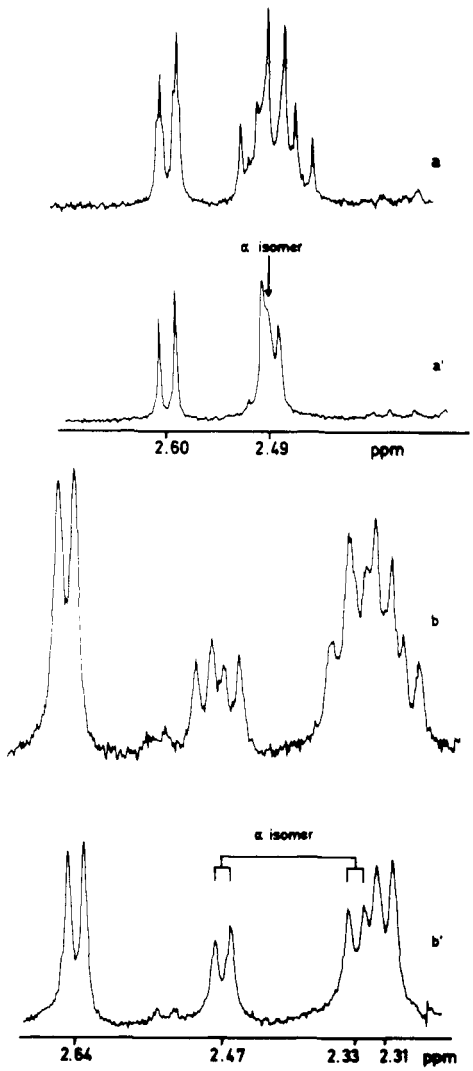

Figure 4. 250-MH ^1H NMR spectra (CD_2Cl_2) of a mixture of the α and β isomers of **2b** ([α]:[β] = 1:2) in the bridging methylene region: (a) at 298 K; (a') $^1H\{^{31}P\}$ at 298 K; (b) at 213 K; (b') $^{31}P\{^1H\}$ at 213 K.

is coupled to two equivalent phosphorus nuclei. The bridging methylene proton signal is temperature dependent, as shown in Figure 4. At 298 K, by decoupling the phosphorus nuclei, the methylene resonances appear at 2.60 and 2.49 ppm, as a typical AB pattern (Figure 4a') with a ca. 4.2 Hz coupling between the geminal protons. Further splittings occur due to PH couplings, and the 12-line pattern shown in Figure 4a is interpreted as the fully resolved AB part of an ABX_2 spin system. The proton resonating at higher chemical shift is weakly coupled (0.8 Hz) to two equivalent phosphorus nuclei whereas the other one is more strongly coupled (7.6 Hz) to two equivalent phosphorus nuceli. We assign the weakly coupled proton, resonating at 2.60 ppm, as H_b and the more strongly coupled proton, resonating at 2.49 ppm, as H_a (see Scheme II) from consideration of relative values of H_a–C–Ir–P and H_b–C–Ir–P torsion angles, as discussed above. At 213 K, the spectrum exhibits essentially similar resonance patterns as at 298 K, which may be similarly interpreted as the AB part of an ABX_2 spin system as expected for a cis isomer in which the methylene protons remain intrinsically nonequivalent whatever the relative disposition of the *tert*-butyl groups. However, the chemical shift difference between each methylene proton is larger as shown in Figure 4b,b'. From 0.11 ppm at 298 K, this difference is 0.33 ppm at 213 K. The modification of the

Scheme III

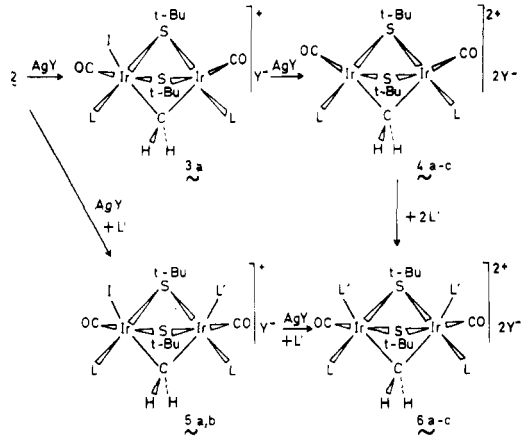

relative disposition of the *tert*-butyl groups of the thiolato bridging ligands is assumed again to be responsible for chemical shift variations.

To sum up, the adduct **2b** exhibits stereoisomerism at the metal atom as well as at the bridging groups. If no dynamic interconversion was detected between cis (α) and trans (β) stereoisomeric forms, the syn–anti interconversion is a fast process at the NMR time scale.

Similar basic structures containing bridging methylene entities and iodide ligands in apical positions, one on each iridium atom, were found from spectroscopic measurements for the other CH_2I_2 adducts **2**, and nonrigidity of the *tert*-butyl groups of the thiolato bridging ligands was observed in each case. Thus, the occurrence of three ν(CO) modes in the IR spectrum of **2a** obviously indicates a retention of the C_{2v} symmetry of the starting material **1a** when CH_2I_2 is added. Moreover, the ^1H NMR spectrum of this adduct, which is temperature-dependent, exhibits in the slow-exchange region two singlets of equal intensities for the *tert*-butyl groups at 1.79 and 1.59 ppm, consistent with an anti relative disposition of these groups. Consequently, the methylene proton resonances appear at 2.57 and 2.45 ppm as a typical AB pattern with a J_{HH} of 5.6 Hz. Upon raising the temperature, the *tert*-butyl groups as well as the methylene protons become equivalent and their resonance signals coalesce into broad singlets.

In cases **2c** and **2d**, only one isomer was formed by oxidative addition of CH_2X_2 to the corresponding materials **1c** and **1d**. As in the α isomer of **2b**, a relative trans disposition of both carbonyl groups and of both phosphine ligands was deduced from NMR data.

As shown in Table VII, the ^{13}C chemical shifts of the μ-CH_2 groups of the CH_2I_2 adducts **2** lie in an unexpected range, from −15 to −35 ppm, if compared with values observed for other complexes in which the methylene ligand bridged two nonbonded metal atoms.[1]

These signals appear as triplets on the ^{13}C NMR spectrum, with $^2J_{CH}$ coupling constants of about 150 Hz, whereas no $^2J_{CP}$ was detected for these complexes, probably owing to the relative cis disposition of phosphine ligands and of the bridging methylene group.

Halide Abstraction Reaction of Complexes 2 by Silver(I) Salts. Complexes **2** are easily dehalogenated in dichloromethane at room temperature, using stoichiometric quantities of silver(I) salts (perchlorate or hexafluorophosphate) leading to dicationic species **4** (Scheme III). Monitored by IR in the case of **2a**, a monocationic intermediate, **3a**, was detected in solution indicating that the reaction proceeds by successive abstraction of each iodide ligand. The dicationic compounds **4** which contain five-coordinated iridium(III) centers are opened to nu-

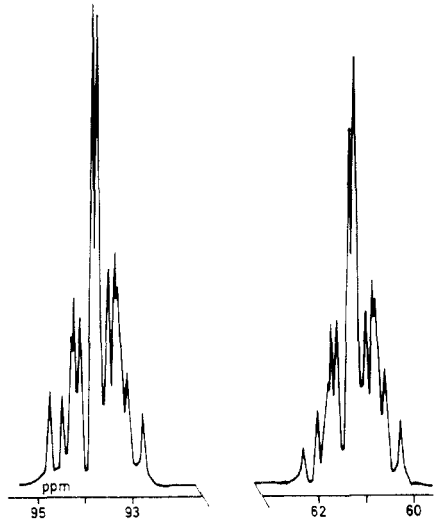

Figure 5. 36.4-MHz $^{31}P\{^1H\}$ NMR spectrum (CD_2Cl_2) of **6b'**.

cleophilic attack, and complexes **6a–c** are quantitatively obtained by addition of tertiary phosphine or carbon monoxide to dichloromethane solutions of the dicationic species **4**. Moreover, when the halide abstraction reaction is accompanied by the addition of tertiary phosphine or carried out under carbon monoxide atmosphere, complexes **6a,b** are obtained quantitatively, whereas monocationic intermediates **5a,b** are detected in solution by IR.

Complexes **6a–c** form air-stable, pale yellow solids which dissolve in dichloromethane, methanol, or tetrahydrofuran but which are insoluble in toluene or petroleum ether. Conductimetric measurements indicate that these complexes are 1:2 electrolytes in methanol solutions.

Spectroscopic studies indicate that the geometry of these complexes can be simply deduced from the geometry of the starting material **2** by the substitution of iodide ligands for the entering nucleophiles. As an example, the iodide abstraction reaction of complex **2a** leading to complex **4a** is accompanied by a shift of ca. 32 cm^{-1} of the three ν(CO) bands toward higher frequencies, and the subsequent addition of triphenylphosphine, leading to **6a**, is accompanied by a shift of ca. 40 cm^{-1} of these bands toward lower frequencies. These observations are indicative of a retention of the relative disposition of the four carbonyl groups in the molecules during the reactions, according to a C_{2v} symmetry. Moreover, the replacement of both iodides ligands by triphenylphosphine in **2a** and by carbon monoxide in **2c** leads significantly to two distinct dications **6a** and **6c** as shown by their IR spectra in the ν(CO) region. The added phosphines in **6a** occupy equivalent positions, as expected.

The $^{31}P\{^1H\}$ NMR spectrum of **6b'** (**6b'** results from the iodide abstraction reaction of a α isomer of **2b** followed by the addition of 2 equivalents of $P(OMe)_3$) exhibits two identical patterns, each pattern containing five pairs of symmetrical lines respectively centered at 93.72 and 61.26 ppm (Figure 5). This is characteristic of an AA'XX' spin system, and it can be analyzed in terms of the parameters K, L, M, and N defined as $K = J_{AA'} + J_{XX'}$, $L = J_{AX} - J_{AX'}$, $M = J_{AA'}, - J_{XX'}$, and $N = J_{AX} + J_{AX'}$. This is fully consistent with the proposed structure which contains one pair of equivalent axial and one pair of equivalent equatorial phosphite ligands. A mutual trans disposition of both equatorial phosphites and of both carbonyl ligands is deduced from the equivalence of the *tert*-butyl groups of the thiolato bridging ligands.

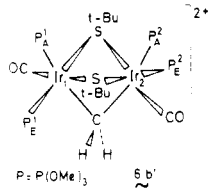

The ^{13}C resonances of the μ-CH_2 group of **6a**, **6b**, **6b'**, and **6c** are shifted considerably toward higher field and lie in a quite unexpected range, i.e., ca. −40 to −65 ppm. The $^{13}C\{^1H\}$ NMR resonances of **6a** and **6b'** appear as triplets with $^2J_{CP}$ coupling constants of 7.3 and 10.5 Hz, respectively.

Acknowledgment. We wish to thank G. Commenges for experimental assistance in NMR and the CNRS for financial support.

Registry No. **1a**, 63312-27-6; **1b**, 63292-76-2; **1c**, 63264-36-8; **1d**, 94890-43-4; **1e**, 63292-79-5; **2a**, 94890-44-5; α-**2b**, 94890-45-6; β-**2b**, 94942-80-0; **2c**, 94890-46-7; **2d**, 94890-47-8; α-**2e**, 94890-48-9; β-**2e**, 94942-81-1; **2f**, 94904-36-6; **3a**, 94890-50-3; **4a**, 94890-52-5; **4b**, 94890-54-7; **4c**, 94890-56-9; **5a**, 94890-58-1; **5b**, 94890-60-5; **6a**, 94890-62-7; **6b**, 94890-64-9; **6b'**, 94890-66-1; **6c**, 94943-28-9; CH_2I_2, 75-11-6; CH_2Br_2, 74-95-3; $[IrI(\mu\text{-}t\text{-}BuS)(CO)(P(OMe)_3)]_2$, 74144-13-1; diazomethane, 334-88-3.

Supplementary Material Available: Tables of observed and calculated structure factors for **2b**, final anisotropic thermal parameters for non-hydrogen atoms, hydrogen positional and thermal parameters, least-squares plane equations (18 pages). Ordering information is given on any current masthead page.